

# Point Discriminative Learning for Unsupervised Representation Learning on 3D Point Clouds

Fayao liu<sup>1</sup> Guosheng Lin<sup>2</sup> Chuan-Sheng Foo<sup>1</sup> Chaitanya K. Joshi<sup>1</sup> Jie Lin<sup>1</sup>

<sup>1</sup>Institute for Infocomm Research, A\*STAR, Singapore <sup>2</sup>Nanyang Technological University

## Abstract

Unsupervised learning has witnessed tremendous success in natural language understanding and 2D image domain recently. How to leverage the power of unsupervised learning for 3D point cloud analysis remains open. Most existing methods simply adapt techniques used in 2D domain to 3D domain, while not fully exploiting the specificity of 3D data. In this work we propose a point discriminative learning method for unsupervised representation learning on 3D point clouds, which is specially designed for point cloud data and can learn local and global shape features. We achieve this by imposing a novel point discrimination loss on the middle level and global level features produced by the backbone network. This point discrimination loss enforces the features to be consistent with points belonging to the corresponding local shape region and inconsistent with randomly sampled noisy points. Our method is simple in design, which works by adding an extra adaptation module and a point consistency module for unsupervised training of the backbone encoder. Once trained, these two modules can be discarded during supervised training of the classifier or decoder for downstream tasks. We conduct extensive experiments on 3D object classification, 3D semantic and part segmentation in various settings and achieve new state-of-the-art results. We also perform a detailed analysis of our method and visually demonstrate that the reconstructed local shapes from our learned unsupervised features are highly consistent with the ground-truth shapes.

## 1. Introduction

Nowadays, due to the increasing demand of 3D applications such as augmented reality (AR), robotic vision, autonomous driving *etc.*, there is a growing surge in 3D related research. Among the various 3D representation methods such as voxels, meshes, implicit functions *etc.*, point clouds have become an increasingly popular option. Point cloud analysis has therefore become an important research area. Learning discriminative and transferrable shape representations is a core problem in most point cloud analysis tasks.

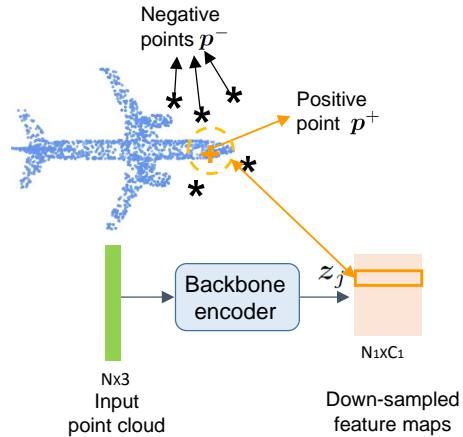


Figure 1. An illustration of our proposed point discriminative learning. An input point cloud is fed to a backbone encoder to get the downsampled feature maps.  $z_j$  is a single feature in the feature maps, which corresponds to a local region (receptive field) in the input point cloud (indicated by the dashed circle). We define input points within this local region as positive points of  $z_j$ . The orange plus marker shows one positive point. We define negative points as randomly sampled noisy points, shown by black stars. Our point discriminative learning trains the backbone encoder in an unsupervised fashion by maximizing consistency scores of  $z_j$  with  $p^+$  while minimizing consistency scores of  $z_j$  with  $p^-$ .

Supervised methods rely on massive labelled data, which causes high annotation costs. In contrast, unsupervised representation learning relies on self-supervision without requiring human labelling. The recent tremendous success achieved by unsupervised representation learning in 2D domain [4, 17, 19] has inspired research on its 3D counterpart.

Various methods for unsupervised representation learning on 3D point clouds have been proposed [1, 15, 16, 29–31, 35, 36, 38, 39, 41, 43]. Most early approaches work by mapping an input point cloud into a global latent representation [21, 31, 39] or a latent distribution in the variational case [15, 16] and then attempting to reconstruct the input. These auto-encoding based methods mostly lack effective exploitation of local geometry for self-supervision, which results in limited performance gain. Recently, re-

search focus has been shifted towards developing various 3D pretext tasks for 3D unsupervised learning. However, due to the less structured characteristic of 3D data, designing such pretext tasks is not as straightforward as in the 2D domain such as predicting image patch orders [24], predicting rotations [10], or colorizing images [42] *etc.* Therefore most existing methods for 3D unsupervised learning simply adapt techniques used in 2D domain to 3D domain. For example, JigSaw3D [30] and Rotation3D [26] are 3D versions of [24] and [10] respectively. More recently, Wang *et al.* [35] propose OcCo by reconstructing partially occluded point clouds as the pretext task, which can be seen as a 3D version of the context encoder method of [25].

Lacking fully exploiting the specificity of 3D data, most existing methods show limited performance improvement. In this work, we propose a point discriminative learning method for 3D unsupervised representation learning, which is specially designed for 3D point clouds. Our motivation is that the learned shape features should be consistent with points from the shape surface and inconsistent with points outside the shape surface. Fig. 1 gives an illustration of our proposed method. For a learned shape feature  $z$ , we regard points within its corresponding input local region (belonging to the shape surface) as positive points and those randomly sampled noises as negative points. We then design a point discrimination loss to maximize the consistency scores of  $z$  with their corresponding positive points, and at meantime minimize the consistency scores of  $z$  with negative points. The consistency scores of features and points are modeled by our point consistency module, which implicitly represents the objects' surface. Due to this novel design of point discriminative learning, our method is especially good at capturing 3D shape geometry, and significantly outperforms previous methods of [30] and [35]. We summarize our contributions in the following:

- We propose a point discriminative learning method PointDisc for unsupervised representation learning on 3D point clouds, which directly exploits the geometric nature of point cloud data. This is achieved by enforcing learned features to be consistent with points belonging to the input point cloud using a point consistency module and a cross-entropy loss.
- We provide detailed analysis of PointDisc and visually demonstrate that the proposed method indeed enforces the learned unsupervised features to capture 3D shape geometry of input point clouds.
- Extensive experiments on 3D classification and segmentation show that our method learns powerful unsupervised representations and can help various downstream 3D learning tasks, achieving new state-of-the-art results.

## 2. Related work

### Unsupervised representation learning on point clouds

Current work can be roughly classified into three categories, *i.e.*, self-reconstruction or auto-encoding based, generative model (*e.g.* GAN) [12] based and self-supervised methods relying on pretext tasks beyond self-reconstruction. Most early methods [1, 15, 16, 21, 29, 39, 43] belong to the first category. These approaches mostly lack effective exploitation of local geometry supervisions, as discussed in [15]. The authors of [15] then propose to capture the local geometry by multi-angle half-to-half prediction. Another line of 3D unsupervised representation learning methods resort to generative models like generative adversarial networks [12] as proposed in [1, 36]. Approaches in the third category rely on pretext tasks beyond self-reconstruction [26, 30, 31], which are attracting more research attention. In [30], the authors propose a pretext task for self-supervision by rearranging randomly shuffled 3D parts. Poursaeed *et al.* [26] propose to predict the rotation angle as the pretext task. Shi *et al.* [31] propose a maximum likelihood estimation method to restore the input point cloud from the one perturbed by Gaussian random noises. Most recently, Wang *et al.* propose OcCo [35], which performs unsupervised representation learning through completing partial point clouds that are manually constructed by occlusion from different view-points. They show that with this simple strategy, the pre-trained model can help a variety of downstream tasks. Their method requires to generate a large partial point cloud dataset for the completion task while we generate unsupervised data on-the-fly for point discriminative learning.

Although demonstrated effective, all the above mentioned methods lack fully exploiting specificity of 3D point cloud data. Different from these approaches, our method is specially designed for 3D point clouds by performing a novel point discriminative learning task for self-supervision. By imposing a novel point discrimination loss on different levels of feature maps produced by the encoder, we directly enforce the learned features to be consistent with global and local geometries of input point clouds. A recent method proposed in [8] learns a maximum likelihood network for probabilistic geometric spatial partition assignments, which also explicitly leverage the geometric nature of point cloud data like our method. In terms of techniques, our method is completely different from [8] in that we perform point discriminative learning while [8] learns discrete generative models for the pretext task.

**Contrastive learning** Contrastive learning [13] has recently become a powerful approach for unsupervised feature learning in the 2D domain [4, 7, 17, 19]. They mainly work by designing a pretext task and then perform dictionary look-up, where a query is enforced to be similar to its positive match and dissimilar to others by optimizing a contrastive loss [17]. Such pretext tasks include exploiting

agreement between examples generated by data augmentation strategies [4, 7], maximizing the mutual information between local patches and global images [19] *etc.* A popular contrastive loss is the InfoNCE [33], which is formulated as a classification problem and implemented with a cross-entropy loss. Our point discrimination loss is also designed as a cross-entropy loss similar to InfoNCE, which is used for maximizing the consistency scores of learned features with positive points in a comparative manner.

In the 3D domain, the authors in [41] propose an object part contrasting method termed as ClusterNet based on graph convolutional neural networks [20] for unsupervised feature learning on point clouds. Their method is trained to determine whether two randomly sampled parts are from the same object. Another contrastive learning method for unsupervised point cloud feature learning using the InfoNCE loss [33] was proposed in [38] and referred as PointContrast. They exploit point cloud correspondences between different views in a data augmentation fashion, which is a common practice used in the 2D domain. Different from ClusterNet [41] and PointContrast [38], we propose a point discriminative learning method to directly enforce the learned features to capture the local and global geometry. This novel design results in powerful unsupervised 3D representations and achieves significantly better results than previous methods.

### 3. Proposed method

Consider  $M$  point clouds  $\{\mathbf{P}_i\}_{i=1,\dots,M}$ , where each  $\mathbf{P}_i \in \mathbb{R}^{N \times 3}$  with each row being a single point  $\mathbf{p}_k \in \mathbb{R}^3$ . Here  $N$  is the total number of points in a single point cloud. We aim to design unsupervised representation learning methods for 3D point clouds. Towards this goal, we propose a point discriminative learning method by maximizing the consistency scores of learned features with positive points belonging to the 3D shape. Meanwhile we minimize the consistency scores of features with randomly sampled negative points. We expect this discrimination task to provide sufficient supervision for learning representations that well capture the global and local shapes. (This claim is supported by our ablation study in Fig. 6.)

#### 3.1. Method overview

Our approach is designed for point-based encoder-decoder style models and we instantiate it on the popular PointNet2 backbone [27]. An overview of our method is shown in Fig. 2. The encoder of the backbone is denoted by the green box while our unsupervised training part is outlined by the red box. The input point cloud is first encoded into a sequence of down-sampled feature maps and then decoded into a category label in the classification task or point-wise predictions in the segmentation task.

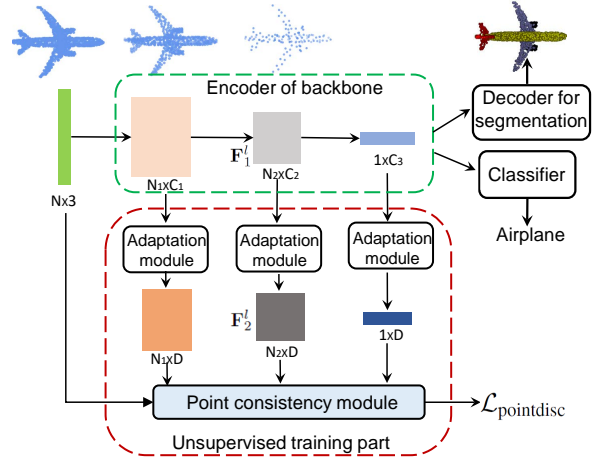


Figure 2. An illustration of our method for unsupervised representation learning on 3D point clouds. Our method works by adding an additional unsupervised training part (red box) to the backbone encoder (green box). It enforces a point discrimination loss on the middle and global level features output by the backbone encoder. This point discrimination loss maximizes the consistency scores of learned features with corresponding points belonging to the local shape. Meanwhile it minimizes consistency scores of learned features with randomly sampled noisy points. Once trained, the unsupervised training part can be discarded during supervised training of the classifier or decoder for down-stream tasks.

We propose a point discriminative learning method to train the backbone encoder in an unsupervised fashion. Specifically, for feature maps produced by the  $l$ -th layer of the backbone encoder  $\mathbf{F}_1^l \in \mathbb{R}^{N_i \times C_l}$ , we first use an adaptation module to map  $\mathbf{F}_1^l$  to a unified dimension  $D$  to obtain new feature maps  $\mathbf{F}_2^l \in \mathbb{R}^{N_i \times D}$ . We then define a point discrimination loss over the features  $\mathbf{z}_j \in \mathbb{R}^D$  in  $\mathbf{F}_2^l$  by discriminating positive points  $\mathbf{p}^+$  from negative points  $\mathbf{p}^-$  conditioning on  $\mathbf{z}_j$ .  $\mathbf{p}^+, \mathbf{p}^- \in \mathbb{R}^3$  are 3 dimensional point coordinates. It is implemented with a point consistency module and a cross-entropy loss. The positive points  $\mathbf{p}^+$  are defined as points that are within the corresponding local region (receptive field) of  $\mathbf{z}_j$  in the input point cloud. Negative points  $\mathbf{p}^-$  are generated by adding random noises to positive points<sup>1</sup>. The proposed unsupervised point discriminative learning enforces learned feature descriptors to be consistent with the local and global geometry of the input point cloud. After the unsupervised training stage, the unsupervised training part can be discarded. We can use the learned encoder as an initialization for supervised training of the whole backbone to perform downstream tasks including point cloud classification and segmentation.

<sup>1</sup>We provide discussions on whether noisy points sampled near the shape surface harm point discriminative learning in Sec. 5

### 3.2. Point discriminative learning

We propose a point discriminative learning method for unsupervised point cloud representation learning. As shown in Fig. 2, this unsupervised loss can be imposed on the middle level and global level point feature maps output by the encoder network. When imposed on the global feature vector, it enforces the learned global feature to capture the overall shape of the input point cloud. We present details of each component of our method in the following.

**Point discrimination loss** We define the point discrimination loss for a training mini-batch as:

$$\mathcal{L}_{\text{pointdisc}} = \sum_{j=1}^{|\mathcal{B}|} \mathcal{L}(z_j). \quad (1)$$

Here  $z_j \in \mathbb{R}^D$  are feature vectors in feature maps  $\mathbf{F}_2^l$  with  $l$  indicating the layer on which we intend to impose our point discrimination loss.  $|\mathcal{B}|$  is the total number of  $z_j$  we use to calculate the loss in one mini-batch.

We define  $\mathcal{L}(z_j)$  by enforcing  $z_j$  to be consistent with positive points  $\mathbf{p}_i^+ \in \mathcal{R}(c_j)$ . Here  $c_j \in \mathbb{R}^3$  denotes the point coordinate associated with  $z_j$  in the downsampled feature map, which corresponds to a local region (receptive field) in the input point cloud.  $\mathcal{R}(c_j)$  is the set of input points that are within a neighborhood of  $c_j$ . To measure the agreement between features and points, we propose a point consistency module  $\text{Cons}(\cdot)$  to output the consistency score.  $\text{Cons}(\cdot)$  is modelled as a neural network with details given next. We then enforce  $\text{Cons}(z_j, \mathbf{p}_i^+)$  to be larger than any  $\text{Cons}(z_j, \mathbf{p}^-)$  with  $\mathbf{p}^-$  being randomly sampled negative points. To achieve this goal, we define  $\mathcal{L}(z_j)$  in a discrimination fashion with the cross-entropy loss:

$$\mathcal{L}(z_j) = -\frac{1}{K} \sum_{i=1}^K \log \frac{\exp(\text{Cons}(z_j, \mathbf{p}_i^+)/\tau)}{\exp(\text{Cons}(z_j, \mathbf{p}_i^+)/\tau) + S^-}, \quad (2)$$

where  $S^- = \sum_{t=1}^T \exp(\text{Cons}(z_j, \mathbf{p}_t^-)/\tau)$ . Here  $K, T$  are the numbers of positive and negative points sampled respectively.  $\tau$  is the temperature hyper-parameter. During implementation, for each point cloud in a single mini-batch, we randomly sample 1000 groups of  $(z_j, \mathbf{p}_1^+, \dots, \mathbf{p}_K^+)$  for calculating the point discrimination loss. Therefore, we have  $|\mathcal{B}| = 1000 \times B$  in Eq. (1) where  $B$  is the training batch size of the input point clouds.

**Point consistency module** The point consistency module  $\text{Cons} : \mathbb{R}^D \times \mathbb{R}^3 \rightarrow \mathbb{R}$  outputs the consistency score of a learned representation  $z$  with a point  $\mathbf{p}$ . We use a neural network to achieve this purpose, shown in Fig. 3. The concatenation  $\hat{z} = [\mathbf{p}, z]$  is used as the network input. Following the architecture used in [3, 23], we first map the input  $\hat{z}$  to a

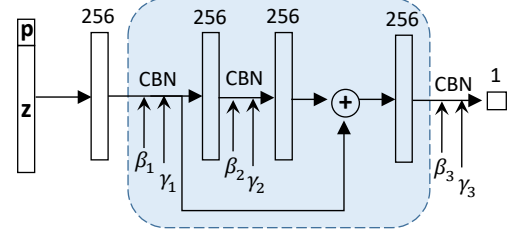


Figure 3. Network architecture of our point consistency module  $\text{cons}(\cdot)$ . The blue box indicates a ResNet module. CBN is the conditional batch normalization [6].

hidden dimension of 256 using a fully connected layer. It is then followed with a pre-activation ResNet block [18] with conditional batch normalization (CBN) [6]. Specifically, the ResNet block consists of two sets of CBN, a ReLU activation layer and a fully-connected (FC) layer with dimension of 256 for the hidden layer. The output of the ResNet block is fed to another set of CBN, ReLU and FC layer to produce the 1-dimensional consistency score, which is used for calculating the point discrimination loss in Eq. 2.

For the CBN module, it takes  $\hat{z}$  as the condition code, which is passed through two FC layers to output the batch normalization parameters, *i.e.*, 256-dimensional vectors  $\gamma(\hat{z})$  and  $\beta(\hat{z})$ . Then for an input  $x$ , the output of CBN is calculated as:

$$\text{CBN}(x) = \gamma(\hat{z}) \frac{x - \mu}{\sigma} + \beta(\hat{z}), \quad (3)$$

where  $\mu$  and  $\sigma$  are the mean and standard deviation of the batch data. Compared with standard BN where  $\gamma$  and  $\beta$  are fixed after learning, here CBN produces dynamic  $\gamma$  and  $\beta$  for different inputs using a neural network. Our experiments show that adding the CBN module leads to more stable training and better generalization. We show this point consistency module design outperforms the one without CBN in the ablation studies in Sec. 5.

**Positive and negative point sets construction** For a particular feature  $z_j$  in the feature maps  $\mathbf{F}_2^l$ , we define its positive points  $\mathbf{p}_i^+$  as the input points that are within a neighborhood region of  $c_j$ . Here  $c_j$  is the point coordinate corresponding to  $z_j$ , which is one of the output by the set abstraction layer in PointNet2. We then conduct ball query with a predefined radius of  $c_j$  to find  $\mathcal{R}(c_j)$ . The negative point set for  $z_j$  is denoted as  $\mathcal{T}(\mathcal{R}(z_j))$  with  $\mathcal{T}(\cdot)$  being a random perturbation operation. We define  $\mathcal{T}(\cdot)$  as adding some random noise  $\epsilon \sim \mathcal{U}[-a, a]$  to the input coordinates.  $\mathcal{U}$  denotes a uniform distribution with  $a$  being a scalar parameter. Gaussian noise can be an alternative option here. We conduct several ablation studies on the negative point set construction strategies in Sec. 5.

## 4. Experiments

### 4.1. Experimental setup

We evaluate our method on 3D object classification, semantic segmentation and part segmentation tasks. Our baseline is PointNet2 with random initializations, referred as “PointNet2+Rand”. We use the single scale grouping (SSG) model for both the baseline and our method.

**Datasets** We conduct 3D object classification on ModelNet [37], ScanObjectNN [32] and ScanNet10 [28]. ModelNet40 and ModelNet10 are composed of CAD models, with each containing 9832/2468 and 3991/908 training/test objects coming from 40 and 10 classes respectively. ScanObjectNN and ScanNet10 are real world datasets containing point cloud scans with occlusions and noises. For semantic segmentation, we use the S3DIS benchmark [2], which consists of point cloud scans from 6 areas covering 271 rooms and 13 semantic classes. For part segmentation, we evaluate on ShapeNetPart [40], which consists of 16881 objects from 16 categories, with each object segmented into 2 to 6 parts. There are 50 parts in total. We follow the standard train/test/val splits for all tasks unless otherwise stated. For evaluation metrics, we use the global accuracy (Acc) for classification and mean Intersection-over-Union (mIoU) for segmentation tasks.

**Implementation details** The adaptation module is designed as a 2-layer multi-layer perceptron (MLP) network with batch normalization and ReLU activation layers. Each layer has a dimension of 256 and the output dimension  $D$  is set to 256. The outputs of the adaptation module are  $L_2$  normalized. For finding  $\mathcal{R}(c_j)$ , we use ball query within a radius which equals to the radius parameter of the grouping layer in PointNet2 [27]. We normalize the input point clouds by centering their bounding boxes to the origin and scaling them to ensure that all points range within the cube  $[-1, 1]^3$  following [3]. The uniform sampling parameter  $a$  for negative points construction is set to 1. We train the model with Adam optimizer and batch size of 24 for 150 epochs. The learning rates for unsupervised pre-training and fine-tuning are initialized as 0.001 and 0.0005 respectively and with exponential decay. The temperature parameter  $\tau$  in Eq. (2) is set to 0.1.

### 4.2. 3D object classification

**Object classification** We first perform object classification on ModelNet40, ScanObjectNN and ScanNet10. We use a single model pre-trained on ModelNet40 as initialization and fine-tune it on each of the 3 datasets. The results are reported over 3 runs and shown in Table 1. Our method performs consistently better than the baseline while outperforming JigSaw3D and OcCo on ScanNet and ScanObjectNN with considerable margins. OcCo achieves the best performance on ModelNet40. We note that in terms of rel-

Method	ModelNet40	ScanNet	ScanObjectNN
DGCNN+Rand [35]	92.5±0.4	76.1±0.7	82.4±0.4
JigSaw3D [30]	92.3±0.3	77.8±0.5	82.7±0.8
OcCo [35]	<b>93.0±0.2</b>	78.5±0.3	83.9±0.4
PointNet2+Rand	91.1±0.4	77.5±0.4	82.1±0.3
<b>PointDisc (Ours)</b>	92.0±0.4	<b>80.1±0.3</b>	<b>86.2±0.3</b>

Table 1. 3D object classification (Acc) on three datasets by pre-training on ModelNet40. The results are reported as mean±ste (standard error) over 3 runs. Our method achieves the best results on ScanNet and ScanObjectNN.

Method	ModelNet40	ModelNet10
T-L Network [11]	74.40	-
3DGAN [36]	83.30	91.00
VSL [22]	84.50	91.00
VIPGAN [14]	91.98	94.05
MRTNet [9]	86.40	-
LGAN <sup>†</sup> [1]	87.27	92.18
LGAN [1]	85.70	95.30
PointCapsNet [43]	88.90	-
FoldingNet <sup>†</sup> [39]	88.40	94.40
FoldingNet [39]	84.36	91.85
ClusterNet [41]	86.80	93.80
Multi-task <sup>†</sup> [16]	89.10	-
MAP-VAE <sup>†</sup> [15]	90.15	94.82
Rotation3D [26]	91.84	-
JigSaw3D <sup>†</sup> [30]	90.69	94.52
ParAE <sup>†</sup> [8]	91.60	-
OcCo [35]	89.20	-
<b>PointDisc (Ours)</b>	<b>92.30</b>	<b>95.37</b>

Table 2. Linear SVM classification (Acc) on ModelNet40 and ModelNet10. Our method outperforms all competing methods. <sup>†</sup> indicates that the model is trained on ShapeNet.

ative accuracy boost over the baseline, our method brings an accuracy improvement of 0.9 compared to 0.5 by OcCo. It is worth noting that our method performs quite well in the cross-dataset setting, *i.e.*, from ModelNet40 to ScanNet and ScanObjectNN. Since ScanNet and ScanObjectNN are real world point cloud datasets with occlusions and noises, this experiment demonstrate that pre-training on CAD models (ModelNet40) with our method can greatly help the recognition of real world datasets.

**Classification with linear SVM** Following the common practice in unsupervised representation learning [8, 29, 30], we also report the results of training a linear support vector machine (SVM) [5] over the features learned by our unsupervised learning method PointDisc. The compared results on ModelNet40 and Model10 are reported in Table 2. As we can see, our method achieves the best results on both datasets, outperforming recent methods [8, 35]. We visualize the feature embeddings of ModelNet10 using tsne [34] in Fig. 4. The model is trained on the ModelNet10 training set and the visualization shows embeddings of the test set.

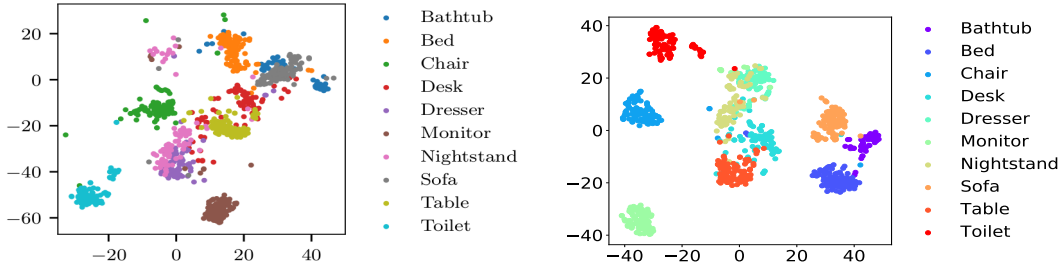


Figure 4. T-SNE [34] visualizations of the unsupervisedly learned features on the ModelNet10 test dataset. Left: JigSaw3D [30] (figure reproduced from the original paper). Right: ours. Our method produces more separable clusters for different categories.

Method	mIoU
DGCNN+Rand [35]	54.9±2.1
JigSaw3D [30]	55.6±1.4 (0.7↑)
OcCo [35]	58.0±1.7 (3.1↑)
PointNet2+Rand	56.1±1.9
<b>PointDisc (Ours)</b>	<b>60.4 ±1.2 (4.3↑)</b>

Table 3. Semantic segmentation results (mIoU) on S3DIS across 6 folds over 3 runs. Our method with PointDisc pre-training achieves the best performance and brings more significant mIoU boost compared to JigSaw3D and OcCo.

The left figure in Fig. 4 shows the visualization result of JigSaw3D [30] (reproduced from the original paper). The right plot shows our result. As we can see, for both methods, the embeddings of “nightstand” and “dresser” are mixed together due to their strong visual similarities. In general, our method produces more separable clusters than [30], which demonstrates strong feature learning capability of our point discriminative learning method.

### 4.3. 3D Semantic segmentation

We further perform experiments on the semantic segmentation task using S3DIS benchmark [2]. Following OcCo [35], we evaluate the 6-fold cross validation performance and report the results in Table 3. Our PointDisc pre-training is performed on the whole training set without labels. As can be seen that our method achieves the best performance and brings more significant mIoU boost over the baseline compared to JigSaw3D and OcCo. We further evaluate another setting by following the original paper of JigSaw3D [30], *i.e.*, pre-training on a large unlabelled set and then fine-tune on a small labelled set, which is more appropriate for demonstrating the benefits of unsupervised pre-training. Specifically, we preserve Area 5 as the test data for all models. For the baseline model, we train on labelled data from different areas except Area 5 with random initialization. For unsupervised pre-training, we pre-train a single model on all areas other than Area 5 without labels, and then fine-tune the model with labelled data from dif-

ferent areas. We run three times and report the mean and standard errors of mIoU scores in Table 4. Compared to JigSaw3D [30], our method achieves the best results in all settings and consistently brings significant mIoU boost over the baseline method. Comparing the results in Table 3 and Table 4, it is worth noting that under limited labelled training data budget as in Table 4, our method shows more performance gains, *i.e.*, generally bringing an absolute mIoU boost of 5.1 to 8.2 points. This fully demonstrates the benefits of unsupervised pre-training for learning with less labelled training data budget.

### 4.4. 3D part segmentation

3D part segmentation is a fine-grained point-wise classification task that requires detailed local geometry features. We conduct experiments on the ShapeNetPart dataset. Following prior works [27, 30], we use the one-hot encoded category label of the object as an extra input for supervised training. During our unsupervised learning, a random class label is given to each object.

Following [38], we first pre-train the encoder with our unsupervised learning method PointDisc on the whole ShapeNetPart training dataset and then fine-tune the encoder and decoder with different percentages of labelled data. The compared mIoU results under different training data budget, *i.e.*, 1%, 5% are reported in Table 5. We mainly compare against PointContrast and other unsupervised learning methods [16, 21, 43] which have reported results under the same setting. To compete with the more powerful SR-UNet backbone, we use multi-scale grouping version of PointNet2. As we can see, our baseline model “PointNet2+Rand” performs even slightly better than the SR-UNet baseline. Overall our method achieves the best performance among all compared methods and brings more significant mIoU boost under both settings. This demonstrates the effectiveness of our unsupervised pre-training method under limited labelled training data budget.

Method	Supervised training area				
	Area 1	Area 2	Area 3	Area 4	Area 6
DGCNN+Rand [30]	43.6	34.6	39.9	39.4	43.9
JigSaw3D [30]	44.7 (1.1 $\uparrow$ )	34.9 (0.3 $\uparrow$ )	42.4 (2.5 $\uparrow$ )	39.9 (0.5 $\uparrow$ )	43.9 (0.0 $\uparrow$ )
PointNet2+Rand	43.0 $\pm$ 0.5	33.7 $\pm$ 0.2	39.5 $\pm$ 0.1	41.0 $\pm$ 0.4	43.5 $\pm$ 0.2
<b>PointDisc (Ours)</b>	<b>50.4<math>\pm</math>0.1 (6.6<math>\uparrow</math>)</b>	<b>39.2<math>\pm</math>0.2 (5.5<math>\uparrow</math>)</b>	<b>47.7<math>\pm</math>0.2 (8.2<math>\uparrow</math>)</b>	<b>46.4<math>\pm</math>0.3 (5.4<math>\uparrow</math>)</b>	<b>48.6<math>\pm</math>0.2 (5.1<math>\uparrow</math>)</b>

Table 4. Semantic segmentation results (mIoU) on S3DIS by testing on Area 5. All the results are obtained by supervised training on different areas and testing on Area 5. We report our results as mean $\pm$ ste (standard error) over 3 runs. Our method with PointDisc pre-training achieves the best performance over all settings and brings much more significant mIoU boost compared to JigSaw3D [30].

Method	1% training	5% training
SONet [21]	64.0	69.0
PointCapsNet [43]	67.0	70.0
Multi-task [16]	68.2	77.7
SR-UNet+Rand [38]	71.8	79.3
PointContrast [38]	74.0 (2.2 $\uparrow$ )	79.9 (0.6 $\uparrow$ )
PointNet2+Rand	72.1 $\pm$ 0.7	79.5 $\pm$ 0.5
<b>PointDisc (Ours)</b>	<b>77.2<math>\pm</math>0.5 (5.1<math>\uparrow</math>)</b>	<b>81.3<math>\pm</math>0.4 (1.8<math>\uparrow</math>)</b>

Table 5. Part segmentation (mIoU) on ShapeNetPart using 1% and 5% labelled training data budgets. Our method (reported as mean $\pm$ ste over 3 runs) outperforms all compared methods and achieves the largest performance gains in both settings.

## 5. Analysis and discussions

In this section, we perform ablation studies for detailed analysis and discussions. Unless otherwise stated, all experiments are conducted by training our PointDisc on the ModelNet40 training set followed by a linear SVM for classification on ModelNet40 test set. The hyperparameter C of SVM is chosen based on a validation set.

**Gaussian noise or uniform noise?** To perform point discriminative learning, we need to sample  $p_t^-$ ,  $t = 1, \dots, T$  to construct the negative point set for each  $z_j$  (see Eq. (2)). We perform a random perturbation on points in  $\mathcal{R}(c_j)$ , where  $\mathcal{R}(c_j)$  denotes the set of positive points. We conduct experiments with two types of noise: uniform and Gaussian. The uniform noise is sampled from  $\epsilon \sim \mathcal{U}[-1, 1]$  while the Gaussian noise is sampled from a standard normal distribution. We perform point discriminative learning with the two different noisy points sampling strategies. Our conclusion is that the uniform noise leads to slightly better result than the Gaussian noise (92.30 vs. 91.82). For all later experiments, we use the uniform noise sampling.

**Do noisy points near the shape surface harm point discriminative learning?** During sampling of negative points, some sampled points may be very close to the local shape surface, which may cause confusion to the point discriminative learning. To figure out this issue, we conduct an ablation study to exclude those points that are within a small distance (0.1) of  $\mathcal{R}(c_j)$ . Our experimental results show that there is no statistically significant difference between mod-

T	1	5	10	20	30
Acc	90.12	91.87	92.30	92.20	92.21

Table 6. Ablation of parameter T on ModelNet40 classification.

Model	l3	l2	l1	CBN	Accuracy (%)
A	✓			✓	90.32
B	✓	✓		✓	91.17
C	✓	✓	✓		91.09
D	✓	✓	✓	✓	<b>92.30</b>

Table 7. Performance comparison of our method using different components. We evaluate the linear SVM classification accuracy on the ModelNet40 dataset.

els with and without this point exclusion strategy. Since the negative points are generated by adding uniform noises to positive points, those near-the-shape-surface points only consist of a small fraction of the sampled points. We conclude that our negative point construction strategy do not bring negative effect to the point discriminative learning.

**Number of positive and negative points per  $z_j$**  We study the effects of sampling different numbers of positive and negative points  $K$ ,  $T$  per  $z_j$  in Eq. (2). For  $K$ , we empirically find that setting  $K$  to larger than 1 converges to similar performance as  $K = 1$ . For  $T$ , we choose it from  $\{1, 5, 10, 20, 30\}$  to train our PointDisc model and then train a linear SVM for classification. We show the results in Table 6. The results show that classification accuracy keeps improving as  $T$  increases from 1 to 10. When  $T$  is set to larger than 10, the performance shows no further gains. We set  $K = 1$  and  $T = 10$  in all our experiments.

**Component analysis** We analyze in detail the contributions of each component in our model with results shown in Table 7. As shown in Fig. 2, our self-supervised point discrimination loss can be imposed on features learned from any intermediate layers or the global level feature (last layer). Our first ablation factor is the contribution of imposing our point discrimination loss on different layers (model A, B, D in Table 7). We use  $l1$ ,  $l2$ ,  $l3$  to indicate the first, second and third layer respectively. Our second ablation factor is the conditional batch normalizatin (CBN) in the

Method	Encoder	Self-supervised module	Total
OcCo [35]	6.66M	6.04M	12.70M
<b>PointDisc (Ours)</b>	0.62M	1.17M	1.79M

Table 8. Comparisons on number of parameters for classification model of OcCo [35] and our PointDisc. Our method is much more lightweight.

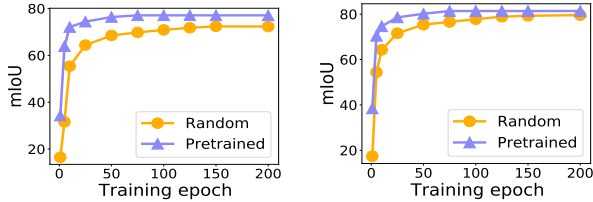


Figure 5. Convergence comparison of random initialized and our pre-trained models on ShapeNetPart segmentation. Left: 1% labeled training data; right: 5% labeled training data.

point consistency module, which is replaced by conventional batch normalization (model C in Table 7). As we can see that imposing the point discrimination loss on more intermediate layers consistently improves the classification performance. Compared to the model without CBN, our full model yields better results which validates the effectiveness of our point consistency module design.

**Model size and convergence analysis** We calculate the number of parameters for the classification model of our method and OcCo [35], with results shown in Table 8. The “Self-supervised module” column shows the number of additional parameters introduced by the self-supervised task of different methods. Our model consists of much less parameters and yet achieves better results as demonstrated in Table 1. The reason is that in OcCo [35], a decoder is required to perform point cloud completion, which is typically large. While our method does not rely on any point cloud reconstruction but a lightweight point consistency module. We show the part segmentation (Table 5) performance in terms of different epochs in Fig. 5 for training from random initialization *vs.* our pre-trained model. The left and right plots show models trained with 1% and 5% labelled data respectively. Compared to random initialization, our pre-trained model leads to much faster convergence and can achieve a decent mIoU score within limited training epochs. The benefit is more significant in the extremely less labelled data scenario, *i.e.*, 1%.

**Visualizing local shapes captured by our learned unsupervised features** After the unsupervised training of PointDisc, for an input point cloud, we can obtain its unsupervised features through the encoder. For a particular  $z$  in the obtained middle-level feature maps, we can visualize the local shape captured by  $z$  through evaluating consistency scores of  $z$  with randomly sampled points. In this

way, we can probe that whether the unsupervised features learned by our PointDisc indeed capture local shapes of the input point cloud. We visualize points with the top 100 highest consistency scores among 5000 uniformly sampled points in Fig. 6. The first row shows input point clouds, with each example showing a centroid (indicated by “+”) and its neighboring region (black circle) corresponding to a learned feature  $z$ . The second row shows ground-truth local shapes. They are positive points corresponding to  $z$  that are used to train our PointDisc. The third row shows local shapes reconstructed from our learned unsupervised feature  $z$ . We can see that the reconstructed local shapes are highly consistent with the ground-truth shapes. This validates our claim that our method learns unsupervised representations which can well capture local 3D shapes.

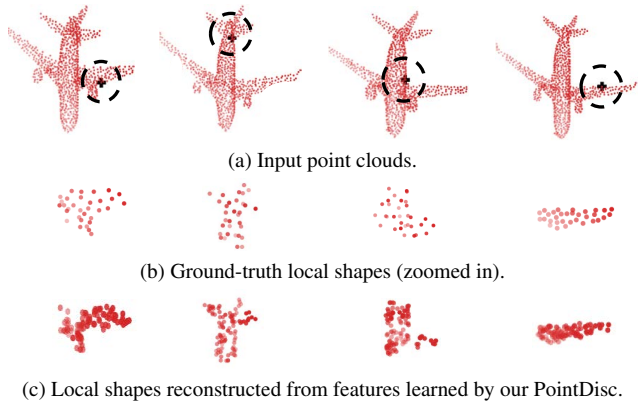


Figure 6. Visualization of reconstructed local shapes from the features learned by our PointDisc. Each of the input point cloud are shown with a centroid (denoted by “+”) and neighboring region (black circle) corresponding to a learned feature  $z$ .

## 6. Conclusion

We propose a novel point discriminative learning method specially designed for unsupervised representation learning on 3D point clouds. By imposing a point discrimination loss on the middle and global level features, our method directly enforces the learned features to capture local and global shape geometry. Extensive experiments on 3D object classification, semantic and part segmentation demonstrate that the propose method has strong feature learning capability, and can be used for pre-training the backbone encoder to improve model performance in downstream tasks. Our work is expected to inspire more research into exploiting the specificity of 3D data for 3D unsupervised learning.

## References

- [1] Panos Achlioptas, Olga Diamanti, Ioannis Mitliagkas, and Leonidas J. Guibas. Learning representations and generative



- models for 3d point clouds. In *ICML*, volume 80, pages 40–49. PMLR, 2018. 1, 2, 5
- [2] Iro Armeni, Ozan Sener, Amir Roshan Zamir, Helen Jiang, Ioannis K. Brilakis, Martin Fischer, and Silvio Savarese. 3d semantic parsing of large-scale indoor spaces. In *CVPR*, pages 1534–1543, 2016. 5, 6
- [3] Ruojin Cai, Guandao Yang, Hadar Averbuch-Elor, Zekun Hao, Serge Belongie, Noah Snavely, and Bharath Hariharan. Learning gradient fields for shape generation. In *ECCV*, 2020. 4, 5
- [4] Ting Chen, Simon Kornblith, Mohammad Norouzi, and Geoffrey E. Hinton. A simple framework for contrastive learning of visual representations. *CoRR*, abs/2002.05709, 2020. 1, 2, 3
- [5] C. Cortes and V. Vapnik. Support vector networks. *Machine Learning*, 20, 1995. 5
- [6] Harm de Vries, Florian Strub, Jérémie Mary, Hugo Larochelle, Olivier Pietquin, and Aaron C. Courville. Modulating early visual processing by language. In *NIPS*, pages 6594–6604, 2017. 4
- [7] Alexey Dosovitskiy, Jost Tobias Springenberg, Martin A. Riedmiller, and Thomas Brox. Discriminative unsupervised feature learning with convolutional neural networks. In *NIPS*, pages 766–774, 2014. 2, 3
- [8] Benjamin Eckart, Wentao Yuan, Chao Liu, and Jan Kautz. Self-supervised learning on 3d point clouds by learning discrete generative models. In *CVPR*, pages 8248–8257, 2021. 2, 5
- [9] Matheus Gadelha, Rui Wang, and Subhransu Maji. Multiresolution tree networks for 3d point cloud processing. In *ECCV*, volume 11211 of *Lecture Notes in Computer Science*, pages 105–122, 2018. 5
- [10] Spyros Gidaris, Praveer Singh, and Nikos Komodakis. Unsupervised representation learning by predicting image rotations. In *ICLR*, 2018. 2
- [11] Rohit Girdhar, David F. Fouhey, Mikel Rodriguez, and Abhinav Gupta. Learning a predictable and generative vector representation for objects. In *ECCV*, volume 9910, pages 484–499, 2016. 5
- [12] Ian J. Goodfellow, Jean Pouget-Abadie, Mehdi Mirza, Bing Xu, David Warde-Farley, Sherjil Ozair, Aaron C. Courville, and Yoshua Bengio. Generative adversarial nets. In *NIPS*, pages 2672–2680, 2014. 2
- [13] Raia Hadsell, Sumit Chopra, and Yann LeCun. Dimensionality reduction by learning an invariant mapping. In *CVPR*, pages 1735–1742, 2006. 2
- [14] Zhizhong Han, Mingyang Shang, Yu-Shen Liu, and Matthias Zwicker. View inter-prediction GAN: unsupervised representation learning for 3d shapes by learning global shape memories to support local view predictions. In *AAAI*, pages 8376–8384. AAAI Press, 2019. 5
- [15] Zhizhong Han, Xiyang Wang, Yu-Shen Liu, and Matthias Zwicker. Multi-angle point cloud-vae: Unsupervised feature learning for 3d point clouds from multiple angles by joint self-reconstruction and half-to-half prediction. In *ICCV*, 2019. 1, 2, 5
- [16] Kaveh Hassani and Mike Haley. Unsupervised multi-task feature learning on point clouds. In *ICCV*, pages 8159–8170, 2019. 1, 2, 5, 6, 7
- [17] Kaiming He, Haoqi Fan, Yuxin Wu, Saining Xie, and Ross B. Girshick. Momentum contrast for unsupervised visual representation learning. In *CVPR*, pages 9726–9735, 2020. 1, 2
- [18] Kaiming He, Xiangyu Zhang, Shaoqing Ren, and Jian Sun. Deep residual learning for image recognition. In *CVPR*, pages 770–778, 2016. 4
- [19] R. Devon Hjelm, Alex Fedorov, Samuel Lavoie-Marchildon, Karan Grewal, Philip Bachman, Adam Trischler, and Yoshua Bengio. Learning deep representations by mutual information estimation and maximization. In *ICLR*, 2019. 1, 2, 3
- [20] Thomas N. Kipf and Max Welling. Semi-supervised classification with graph convolutional networks. In *ICLR*. OpenReview.net, 2017. 3
- [21] Jiaxin Li, Ben M. Chen, and Gim Hee Lee. So-net: Self-organizing network for point cloud analysis. In *CVPR*, pages 9397–9406, 2018. 1, 2, 6, 7
- [22] Shikun Liu, C. Lee Giles, and Alexander Ororbia. Learning a hierarchical latent-variable model of 3d shapes. In *ICDV*, pages 542–551, 2018. 5
- [23] Lars M. Mescheder, Michael Oechsle, Michael Niemeyer, Sebastian Nowozin, and Andreas Geiger. Occupancy networks: Learning 3d reconstruction in function space. In *CVPR*, pages 4460–4470, 2019. 4
- [24] Mehdi Noroozi and Paolo Favaro. Unsupervised learning of visual representations by solving jigsaw puzzles. In *ECCV*, volume 9910, pages 69–84, 2016. 2
- [25] Deepak Pathak, Philipp Krähenbühl, Jeff Donahue, Trevor Darrell, and Alexei A. Efros. Context encoders: Feature learning by inpainting. In *CVPR*, pages 2536–2544, 2016. 2
- [26] Omid Poursaeed, Tianxing Jiang, Han Qiao, Nayun Xu, and Vladimir G. Kim. Self-supervised learning of point clouds via orientation estimation. In Vitomir Struc and Francisco Gómez Fernández, editors, *3DV*, pages 1018–1028, 2020. 2, 5
- [27] Charles Ruizhongtai Qi, Li Yi, Hao Su, and Leonidas J. Guibas. Pointnet++: Deep hierarchical feature learning on point sets in a metric space. In *NIPS*, pages 5099–5108, 2017. 3, 5, 6
- [28] Can Qin, Haoxuan You, Lichen Wang, C.-C. Jay Kuo, and Yun Fu. Pointdan: A multi-scale 3d domain adaption network for point cloud representation. In Hanna M. Wallach, Hugo Larochelle, Alina Beygelzimer, Florence d’Alché-Buc, Emily B. Fox, and Roman Garnett, editors, *NIPS*, pages 7190–7201, 2019. 5
- [29] Yongming Rao, Jiwen Lu, and Jie Zhou. Global-local bidirectional reasoning for unsupervised representation learning of 3d point clouds. In *CVPR*, pages 5375–5384, 2020. 1, 2, 5
- [30] Jonathan Sauder and Bjarne Sievers. Self-supervised deep learning on point clouds by reconstructing space. In *NIPS*, pages 12942–12952, 2019. 1, 2, 5, 6, 7

- [31] Yi Shi, Mengchen Xu, Shuaihang Yuan, and Yi Fang. Unsupervised deep shape descriptor with point distribution learning. In *CVPR*, pages 9350–9359, 2020. 1, 2
- [32] Mikaela Angelina Uy, Quang-Hieu Pham, Binh-Son Hua, Duc Thanh Nguyen, and Sai-Kit Yeung. Revisiting point cloud classification: A new benchmark dataset and classification model on real-world data. In *ICCV*, pages 1588–1597, 2019. 5
- [33] Aäron van den Oord, Yazhe Li, and Oriol Vinyals. Representation learning with contrastive predictive coding. *CoRR*, abs/1807.03748, 2018. 3
- [34] L.J.P. Van der Maaten and G.E. Hinton. Visualizing high-dimensional data using t-sne. 2008. 5, 6
- [35] Hanchen Wang, Qi Liu, Xiangyu Yue, Joan Lasenby, and Matt J. Kusner. Unsupervised point cloud pre-training via occlusion completion. In *ICCV*, 2021. 1, 2, 5, 6, 8
- [36] Jiajun Wu, Chengkai Zhang, Tianfan Xue, Bill Freeman, and Josh Tenenbaum. Learning a probabilistic latent space of object shapes via 3d generative-adversarial modeling. In *NIPS*, pages 82–90, 2016. 1, 2, 5
- [37] Zhirong Wu, Shuran Song, Aditya Khosla, Fisher Yu, Linguang Zhang, Xiaoou Tang, and Jianxiong Xiao. 3d shapenets: A deep representation for volumetric shapes. In *CVPR*, pages 1912–1920. IEEE Computer Society, 2015. 5
- [38] Saining Xie, Jiatao Gu, Demi Guo, Charles R Qi, Leonidas J Guibas, and Or Litany. Pointcontrast: Unsupervised pre-training for 3d point cloud understanding. 2020. 1, 3, 6, 7
- [39] Yaoqing Yang, Chen Feng, Yiru Shen, and Dong Tian. Foldingnet: Point cloud auto-encoder via deep grid deformation. In *CVPR*, pages 206–215. IEEE Computer Society, 2018. 1, 2, 5
- [40] Li Yi, Vladimir G. Kim, Duygu Ceylan, I-Chao Shen, Mengyan Yan, Hao Su, Cewu Lu, Qixing Huang, Alla Sheffer, and Leonidas J. Guibas. A scalable active framework for region annotation in 3d shape collections. *ACM Trans. Graph.*, 35(6):210:1–210:12, 2016. 5
- [41] Ling Zhang and Zhigang Zhu. Unsupervised feature learning for point cloud understanding by contrasting and clustering using graph convolutional neural networks. In *ICDV*, pages 395–404, 2019. 1, 3, 5
- [42] Richard Zhang, Phillip Isola, and Alexei A. Efros. Colorful image colorization. In Bastian Leibe, Jiri Matas, Nicu Sebe, and Max Welling, editors, *ECCV*, volume 9907, pages 649–666, 2016. 2
- [43] Yongheng Zhao, Tolga Birdal, Haowen Deng, and Federico Tombari. 3d point capsule networks. In *CVPR*, pages 1009–1018, 2019. 1, 2, 5, 6, 7